ACS OMEGA

http://pubs.acs.org/journal/acsodf

Article

Development of a Cell-Based AlphaLISA Assay for High-Throughput Screening for Small Molecule Proteasome Modulators

Sophia D. Staerz, Erika M. Lisabeth, Evert Njomen, Thomas S. Dexheimer, Richard R. Neubig, and Jetze J. Tepe*

Cite This: *ACS Omega* 2023, 8, 15650−15659

Read Online

ACCESS | Metrics & More | Article Recommendations | Supporting Information

ABSTRACT: The balance between protein degradation and protein synthesis is a highly choreographed process generally called proteostasis. Most intracellular protein degradation occurs through the ubiquitin−proteasome system (UPS). This degradation takes place through either a ubiquitin-dependent or a ubiquitin-independent proteasomal pathway. The ubiquitin-independent pathway selectively targets unfolded proteins, including intrinsically disordered proteins (IDPs). Dysregulation of proteolysis can lead to the accumulation of IDPs, seen in the pathogenesis of various diseases, including cancer and neurodegeneration. Therefore, the enhancement of the proteolytic activity of the 20S proteasome using small molecules has been identified as a promising pathway to combat IDP accumulation. Currently, there are a limited number of known small molecules that enhance the activity of the 20S proteasome, and few are observed to exhibit enhanced proteasome activity in cell culture. Herein, we describe the development of a high-throughput screening assay to identify cell-permeable proteasome enhancers by utilizing an AlphaLISA platform that measures the degradation of a GFP conjugated intrinsically disordered protein, ornithine decarboxylase (ODC). Through the screening of the Prestwick and NIH Clinical Libraries, a kinase inhibitor, erlotinib, was identified as a new 20S proteasome enhancer, which enhances the degradation of ODC in cells and α-synuclein *in vitro*.

INTRODUCTION

Proteostasis is a highly orchestrated balance between protein synthesis and degradation.[1,2] This process is regulated through the cross-coordination of several cellular pathways, including the ubiquitin−proteasome system (UPS).[2−7] The UPS is a vital protein degradation system and is responsible for the degradation of most intracellular and soluble proteins.[3,7] The main protease of the UPS is the enzymatic core particle: the 20S proteasome.[3,4,7,8] The 20S proteasome is barrel-shaped and composed of four stacked heptameric rings where the two α-rings sandwich the two β-rings.[7,8] The β-rings house the three catalytic sites: the β_1 (caspase-like), β_2 (trypsin-like), and β_5 (chymotrypsin-like).[7−9] Access to these catalytic sites is controlled by the amino termini pendant groups of the α-rings that interlace to form a gate to the interior of the 20S core particle. Regulatory particles, like the 19S cap, can dock into pockets between the α-rings and induce an open-gate 20S conformation. This assembled complex (19S-20S-19S or 19S-20S) is referred to as the 26S proteasome.[7,8] The 19S caps recognize and unfold ubiquitinylated proteins, cleave their ubiquitin tags, and translocate the linearized proteins into the 20S core particle for their proteolytic degradation.[8] The standalone 20S proteasome can directly degrade proteins that are inherently unfolded, such as intrinsically disordered proteins (IDPs) or oxidatively damaged proteins, in a ubiquitin-independent manner due to continuous gate oscillation between an open and closed conformation.[10,11]

IDPs are a class of proteins that contain large peptide regions that lack a stable three-dimensional (3D) conformation.[12,13] This dynamic nature allows IDPs to have several different binding partners. Due to this flexibility, they require a high degree of regulation to avoid unwanted side interactions.[14] However, because of age-related decline in UPS activity,[1] genetic factors,[15] or a combination of the two, the expression rate of IDPs can outpace their degradation, perturbing proteostasis.[16] Some IDPs readily aggregate during this disruption, as seen in neurogenerative diseases, including Alzheimer's and Parkinson's Diseases.[17] During this aggregation process, toxic oligomeric species are formed that can inhibit the proteasome, propagating a noxious cycle of enhanced protein accumulation.[16] Accumulation of other IDPs, such as the transcription factor MYC, can cause unregulated transcription of many tumor-promoting genes.[18,19]

Received: February 20, 2023
Accepted: April 12, 2023
Published: April 21, 2023

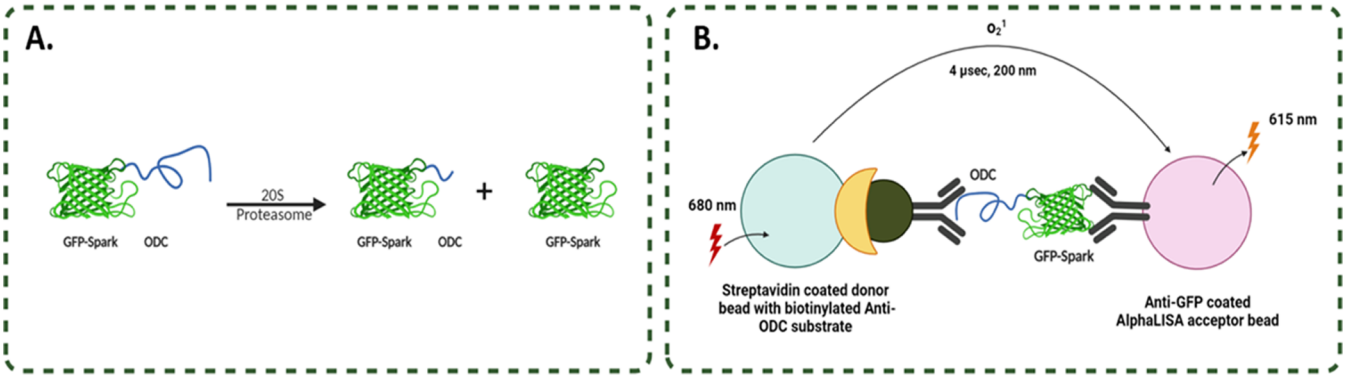

Figure 1. (A) Schematic of theorized cleavage pattern of the GFP-ODC conjugated protein by the 20S proteasome and (B) the interaction between the donor and acceptor beads when brought together by the GFP-ODC conjugated protein.

IDPs have become a focus in the development of therapeutics for a range of diseases, yet the innate flexibility of these proteins poses a significant obstacle in the development of direct small molecule modulators.[12,13] Preventing IDP accumulation by enhancing the proteolytic activity of the 20S proteasome using small molecules and peptides is therefore considered a promising alternative.[20−27] While there has been significant progress in the development of small molecule and peptide 20S proteasome enhancers, the chemical space is limited, and few molecules display potent cellular activity. Novel classes of 20S proteasome enhancers must be identified to further evaluate this new therapeutic strategy in cell models and *in vivo*. To address this need, cellular activity assays must be developed to meet the demands of high-throughput screening.

Standard proteasome activity measurement assays utilize a modified small peptide substrate that is conjugated to a 4-amino-7-methylcoumarin (AMC) probe.[28] Although these AMC probes are valuable tools, their small size allows them to enter the 20S proteasome core without the gate being fully open, leading to poor sensitivity.[29] Furthermore, these probes are not cell permeable, limiting their use to cell lysates or purified enzymatic assays.[30] With these limitations in mind, Forster resonance energy transfer (FRET)-based probes were designed to evaluate proteasome activity *in vitro*.[31] The sensitivity of these probes makes them an ideal choice for high-throughput assays when using purified 20S proteasome.[32] However, similarly to the AMC probes, these probes are not cell permeable, limiting their use to examining purified proteasomal activity.[30,32] In addition, small peptide probes are designed to mimic the preferred cleavage site of each proteasomal catalytic site.[29] To evaluate the overall proteasome activity, all three probes must be used in combination. Furthermore, the protocols of proteasome inhibition and proteasome enhancement often differ drastically. For example, the proteasome must be artificially activated with a detergent, like sodium dodecyl sulfate (SDS), to test for proteasome inhibition.[33] Lastly, the proteolytic degradation of these small peptide probes (with 3−5 amino acids) does not necessarily recapitulate the endogenous proteosome-mediated degradation of full-size proteins. To address these shortcomings, we sought to develop a cellular high-throughput assay capable of detecting small molecules that induce 20S proteasome-mediated degradation of intact intrinsically disordered proteins.

The two-bead assay, AlphaLISA (amplified luminescent proximity homogeneous assay), provides an ideal platform to address this need due to its high sensitivity and ease of modification. Herein, we describe the development of a cell-based AlphaLISA designed to measure the proteolytic degradation of a well-known IDP, ornithine decarboxylase (ODC), that is conjugated with a green fluorescent protein (GFPSpark) on its N-terminus (Figure 1A).[23] Compared to other GFP types, GFPSpark folds more quickly and maintains its exceptionally stable β-barrel structure, giving it a high degree of stability that proves difficult for even the 19S cap's unfolding abilities to overcome.[34] ODC is a homodimeric enzyme that plays a key role in the biosynthesis of polyamines. In its monomeric form, ODC is inactive, intrinsically disordered, and can be degraded by the 20S proteasome.[23,35] The opposing structural characteristics of GFPSpark and ODC make their conjugated protein combination an ideal substrate for the evaluation of 20S proteasome modulation by small molecules. Utilization of this cell-based AlphaLISA enabled us to screen the NIH Clinical Library and the Prestwick Library, identifying erlotinib as a new 20S proteasome enhancer.

RESULTS AND DISCUSSION

Development of GFP-ODC AlphaLISA Assay. AlphaLISA assays rely on an electron transfer between two beads: a donor and an acceptor bead.[36−38] When the donor bead is excited with 680 nm of light, a singlet oxygen species is produced.[36,37,39] This oxygen species can travel approximately 200 nm and add across an alkene double bond of a thioxene derivative on the acceptor bead.[38] The energy released during this reaction then excites a Europium chelate, ultimately emitting a signal around 615 nm.[36,37,39] However, if the acceptor bead is not within 200 nm, this reaction will not occur, and no signal will be emitted at 615 nm (Figure 1B).

This distance dependency is advantageous in the development of a proteasome activity assay. Here, the donor bead was coated with streptavidin and conjugated with a biotinylated anti-ODC antibody, while the acceptor bead was coated with an anti-GFP antibody. When the full-length conjugated protein is present, the two beads are brought together, causing the AlphaLISA signal observed at 615 nm. In a cellular setting, the 20S proteasome can readily degrade the ODC portion of the conjugated protein, lowering the concentration of the full-length GFP-ODC in the cell lysate. This prevents the beads from being kept within 200 nm, resulting in a decrease of the emission signal at 615 nm. Thus, when a proteasome

https://doi.org/10.1021/acsomega.3c01158
ACS Omega 2023, 8, 15650−15659

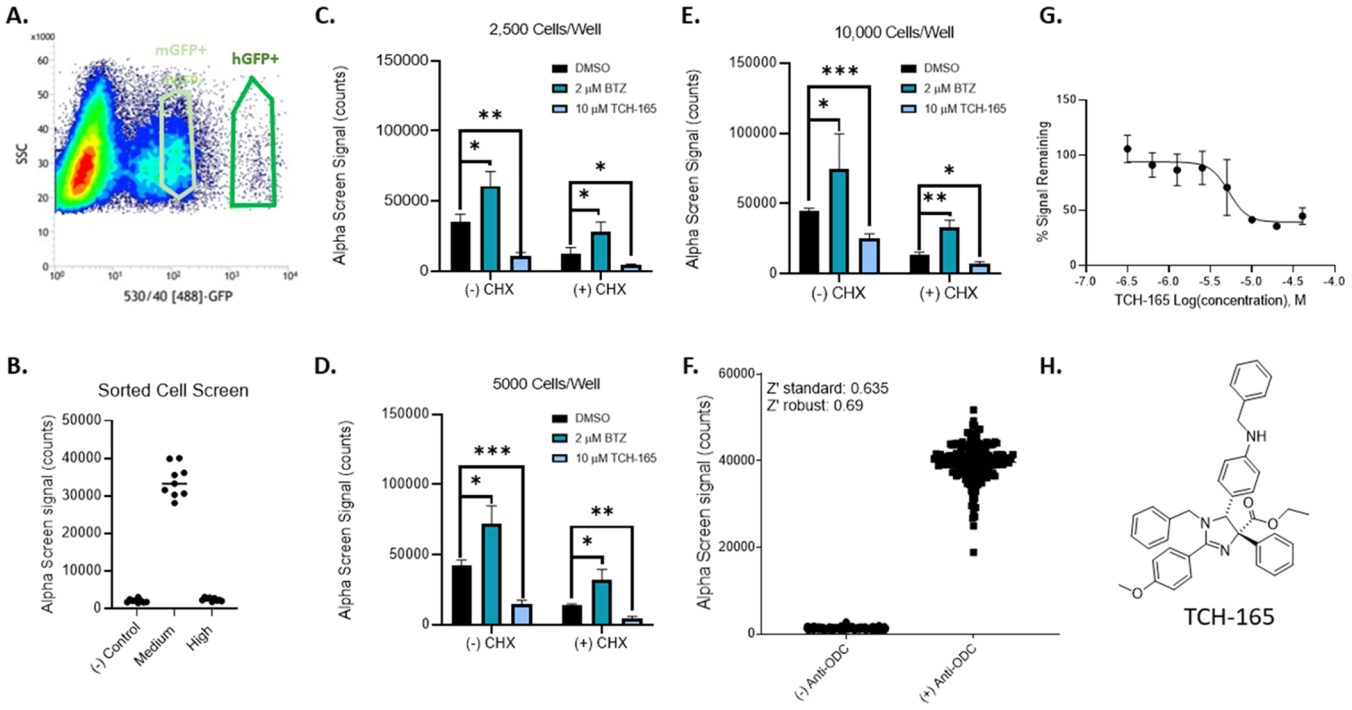

Figure 2. (A) Distribution of GFP expressors sorted using flow cytometry. The lighter green box represents cells that display a "medium" GFP signal (mGFP$^+$), while the dark green box is the cells that display a "high" GFP signal (hGFP$^+$). (B) AlphaLISA signal of each of the cell populations. AlphaLISA signal of (C) 2500 cells/well, (D) 5000 cells/well, and (E) 10,000 cells/well when treated with dimethyl sulfoxide (DMSO), 10 μM TCH-165, and 2 μM BTZ in two conditions, with and without cycloheximide (CHX) one-way ANOVA statistical analysis was used to determine statistical significance. (ns = not significant, *$p < 0.05$, **$p < 0.01$, ***$p < 0.001$, ****$p < 0.0001$). (F) Sample distribution from a full 384-well plate to examine the Z'-score, which was calculated to be 0.635. (G) Dose−response inhibition of the AlphaLISA signal by TCH-165. Data were graphed with GraphPad Prism 9 [Nonlinear regression: log agonist vs response-variable slope (4 parameters)] (H) Structure of TCH-165.

modulator is introduced, the degree to which ODC is proteolytically degraded will be readily altered. If a proteasome inhibitor is present, there should be an increase of the AlphaLISA signal compared to the signal resulting from the basal degradation of untreated proteasomes. Inversely, if a proteasome enhancer is in the system, the signal should decrease compared to the untreated control due to enhanced proteolysis of ODC.

Prior to evaluating proteasome modulators, the AlphaLISA assay was optimized to ensure that the signal was stable and reproducible. To screen the concentrations of both beads and the antibodies needed for the highest and most consistent AlphaLISA signal, HEK-293T cells transiently expressing GFP-ODC were used. Cells were seeded at 1000 cells/well in white, opaque bottom, 384-well plates. After a 12 h incubation, to allow the cells to adhere and recover from the plating process, the cells were directly lysed in the assay plate, and eight different combinations of concentrations of the acceptor bead (10 or 5 μg/mL), streptavidin donor bead (40 or 20 μg/mL), and the biotinylated anti-ODC antibody (1 or 3 nM) were screened (Figure S1). Cell lysates not treated with the biotinylated anti-ODC antibody serve as the negative control. The AlphaLISA signal of each condition was then compared to this negative control. All of the combinations produced a significant signal-to-noise ratio over the negative control; however, cell lysates treated with 10 μg/mL anti-GFP acceptor bead, 40 μg/mL Streptavidin donor bead, and 3 nM of the biotinylated anti-ODC antibody displayed the highest signal-to-noise ratio of 41 over the negative control. These conditions were carried forward to optimize cell type and number.

While the transiently transfected cell line produced a high signal-to-noise ratio, a stable cell line would ensure signal stability and reproducibility. Furthermore, a stable cell line would be needed to adapt this assay for high-throughput screening. Using flow cytometry, a pool of HEK-293T cells that were stably transfected with the GFP-ODC construct were sorted into medium (light green box) and high GFP (dark green box) expressors (Figure 2A). The resulting cell populations were seeded at 2500 cells/well in the white 384-well plates. The AlphaLISA was performed using the previously optimized bead concentration. Interestingly, the cells that expressed high levels of GFP did not produce any AlphaLISA signal (Figure 2B), while the medium expressors displayed a significant signal-to-noise ratio of 15. At substantially high concentrations of the analyte (GFP-ODC), non-productive complexes can be formed, *i.e.*, GFP-bound beads or ODC-bound beads only but not the ternary complex, also referred to as the Hook effect.

Using the "pool of medium expressers," the optimal number of cells/well was determined (Figure 2C−E). The HEK-293T cells were seeded at 2500 cells/well, 5000 cells/well, and 10,000 cells/well in a white 384-well plate. As the cells were plated, samples from each seeding condition were also treated with a proteasome inhibitor, Bortezomib (BTZ), and a known 20S proteasome enhancer, TCH-165.[23] These samples were included to identify which cell number would produce the most significant signal difference between the proteasome modulators and the untreated vehicle. In parallel, we conducted the assay with and without cycloheximide (CHX)

https://doi.org/10.1021/acsomega.3c01158
ACS Omega 2023, 8, 15650−15659

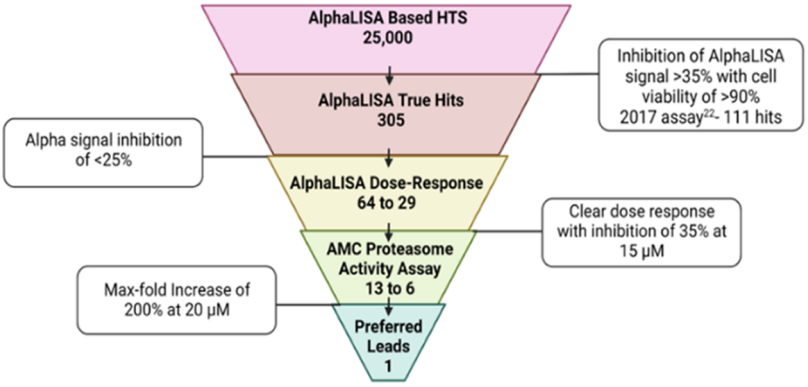

Figure 3. Screening funnel for the screening of the Prestwick and NIH Clinical Libraries, which consist of 2000 compounds, using the optimized AlphaLISA.

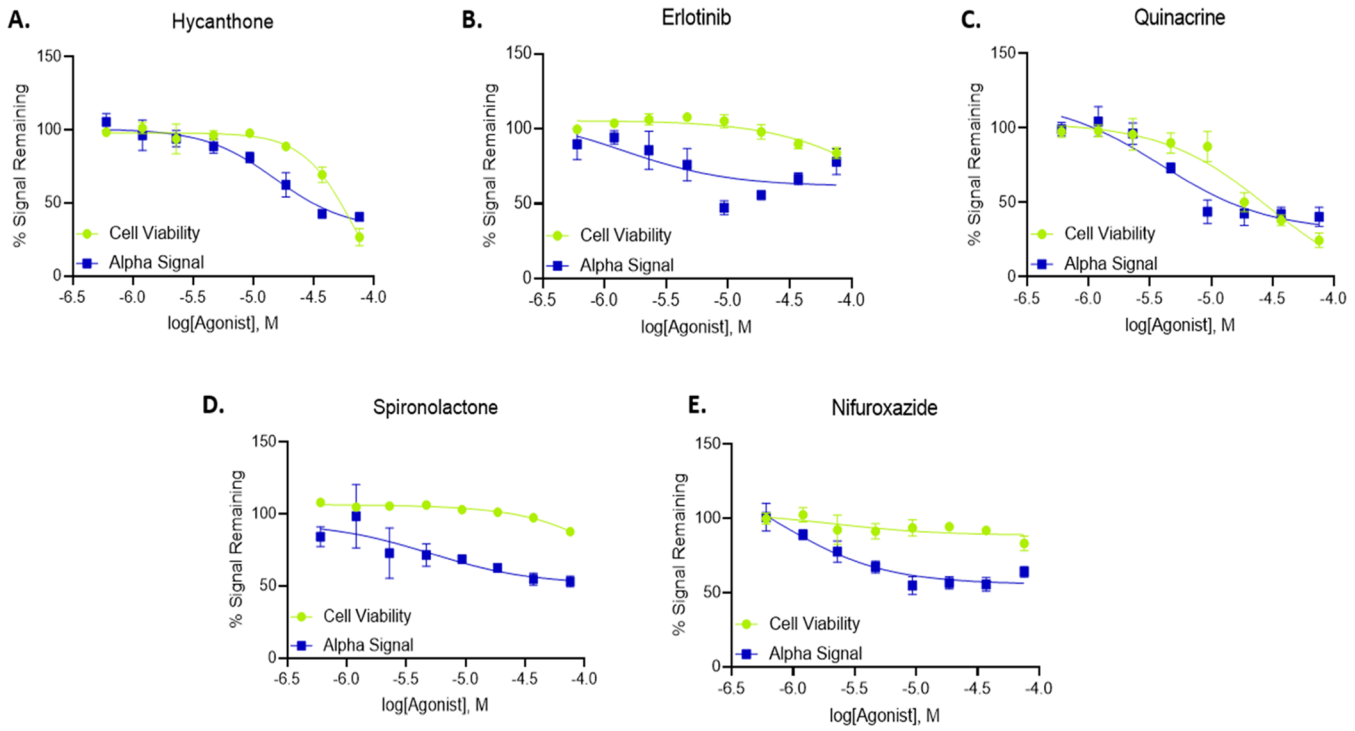

Figure 4. 8-point dose−response curves of (A) hycanthone, (B) erlotinib, (C) quinacrine, (D) spironolactone, and (E) nifuroxazide. The green line represents cell viability, and the blue line represents percent of the AlphaLISA signal; data were graphed with GraphPad Prism 9 [Nonlinear regression: log agonist vs response-variable slope (3 parameters)].

to visualize if halting protein production is needed to observe a significant effect by proteasome modulators (Figure 2C−E).

While all three seeding conditions displayed a high AlphaLISA signal, the non-CHX-treated samples seeded at 10,000 cells/well displayed a signal-to-noise ratio of 23 over the negative control, making these seeding conditions optimal (Figure 2E). In comparison, the CHX-treated samples seeded at 10,000 cell/well only had a signal-to-noise ratio of 6. The percent change observed with the proteasome inhibitor, BTZ, and the proteasome activator, TCH-165,[23] were comparable between the CHX-treated and non-treated cells. Therefore, eliminating the addition of CHX streamlines the assay's workflow without affecting the magnitude that the proteasome modulators have on the AlphaLISA signal.

Upon optimization of the AlphaLISA, we executed a Z' test to evaluate the robustness of the assay, allowing for validation that the AlphaLISA could be employed in a high-throughput screen. A Z' test measures the Z' factor, which is a function of assay quality. This factor describes the separation between the positive and negative control, giving an indication of the likelihood of false negatives or positives.[40] Assays that have a Z' factor of 0.5 or higher are considered to be excellent candidates for high-throughput screening. The AlphaLISA assay was carried out in a white 384-well plate, and half of the wells were not treated with the biotinylated anti-ODC antibody to act as our negative control. The Z' factor was determined using the data collected from these experiments (Figure 2F). The robust Z' factor, using the median values and median absolute deviation, was calculated to be 0.69, indicating the high reproducibility and robustness of the assay. The robust Z' factor reduces the influence of outliers, while the standard Z' factor equation would have to be manually manipulated to account for them.[40,41] While the Z' factor was excellent, we still needed to validate a dose−

https://doi.org/10.1021/acsomega.3c01158
ACS Omega 2023, 8, 15650−15659

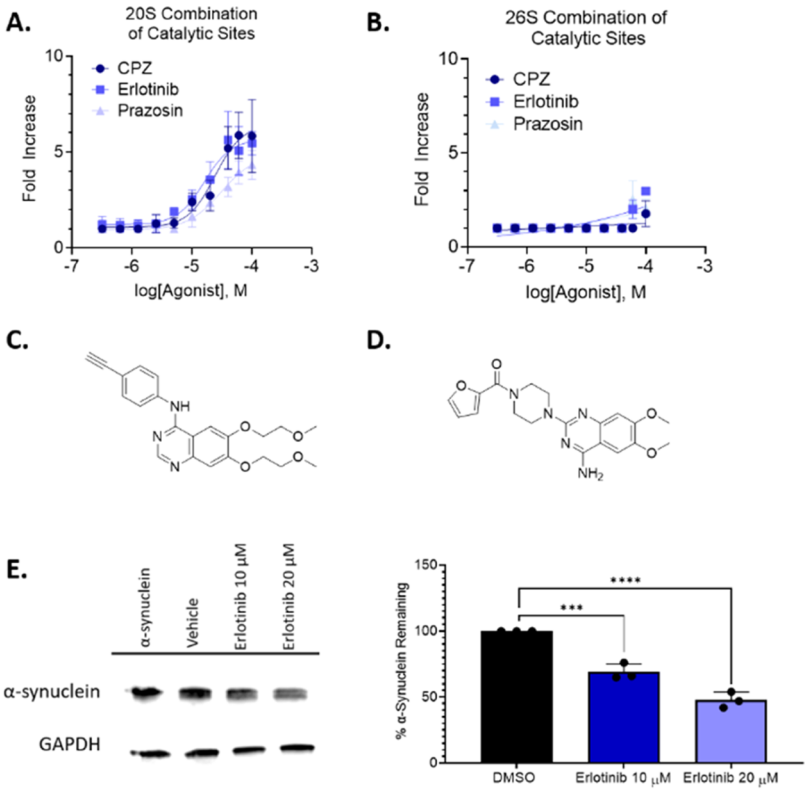

Figure 5. (A) Activation of the overall 20S proteasome using combination catalytic sites. Only prazosin and erlotinib displayed any activation, along with the control, CPZ. (B) Activation of the 26S proteasome when treated with erlotinib, prazosin, and CPZ. The structures of (C) erlotinib and (D) prazosin. (E) Proteolytic degradation of purified α-synuclein by the 20S proteasome when treated with DMSO or erlotinib (10 or 20 μM). One-way ANOVA statistical analysis was used to determine statistical significance (ns = not significant, *$p < 0.05$, **$p < 0.01$, ***$p < 0.001$, ****$p < 0.0001$), with error bars denoting SD. Both A and C graphs were fitted with a log (inhibitor) vs response (four parameters).

response signal decrease with a proteasome activator, TCH-165 (Figure 2G). Using optimized conditions, the assay produced a clear dose−response decrease when subjected to a range of TCH-165 concentrations, resulting in an IC_{50} of 10 μM (Figure 2G). With these studies, we deemed the assay optimized and ready to use in a 2000-compound screen.

Screening of the Prestwick and NIH Clinical Libraries and Hit Validation. With the successful development of the AlphaLISA and the validation of its reproducibility and robustness, the Prestwick and the NIH Clinical compound libraries were screened. Prior to beginning the screen, we established the criteria required for a molecule to be considered a hit: compounds that reduced the AlphaLISA signal by >35% with >90% cell viability in a parallel CellTiter-Glo assay. We also established the orthogonal assays needed to evaluate the hit compounds and the activity that they must exhibit to be considered a lead compound (Figure 3). The AlphaLISA was performed using the optimized conditions, and once the cells were plated in a white 384-well plate, we immediately treated the samples with 15 μM of each of the test compounds for 16 h. From the 2000 compounds screened from the two libraries, 62 were able to lower the AlphaLISA signal by 35% while maintaining at least 90% cell viability and were carried forward.

To eliminate false positives, we used a TrueHits assay to evaluate the interaction of the 62 compounds with the AlphaLISA signal itself. Compounds that inhibited the AlphaLISA signal by 25% or more were removed, leaving 36 compounds. These 36 compounds were then evaluated in a GFP-ODC AlphaLISA using an 8-point titration (80−0.625 μM) using solutions made from the original library compound plates.

Of the 36 compounds, 11 displayed a 35% inhibition of the GFP-ODC AlphaLISA signal at 15 μM. Fresh powder stocks of these 11 compounds and a 20S activator identified in our 2017 screen,[22] chlorpromazine (CPZ), were then evaluated again in an 8-point GFP-ODC AlphaLISA (Figures 4 and S2). CPZ was used as a direct way to compare a successful lead identified in the 2017 high-throughput screen and our novel cell-based high-throughput screen.[22] Due to the continuous production of GFP-ODC, the signal was never reduced to baseline by the compounds.

From the 11 compounds and CPZ, only 5 compounds displayed a reduction in the GFP-ODC AlphaLISA signal that could not be directly attributed to a decrease in cell number (Figure 4). Hycanthone, a frameshift mutagen used to treat schistosomiasis,[42] displayed an IC_{50} of the AlphaLISA signal of 15.1 μM with a CC_{50}, or the concentration at which there is 50% cell death, of 69.7 μM (Figure 4A). The EGFR kinase inhibitor,[43] erlotinib, displayed a promising dose response in the AlphaLISA, with no significant cell cytotoxicity (Figure 4B) but did display poor solubility at higher concentrations. An extended and narrower dose response was conducted for erlotinib, and an IC_{50} of 5.4 μM was identified (Figure S2). Quinacrine, an antimalarial medication,[44] was more cytotoxic with a CC_{50} of 16.0 μM but displayed a similar potency in the AlphaLISA as erlotinib (IC_{50} of 4.8 μM, Figure 4C). The last two compounds, a commonly used mineralocorticoid and androgen receptor antagonist, spironolactone,[45] and an antibiotic, nifuroxazide,[46] showed a decrease in the AlphaLISA

https://doi.org/10.1021/acsomega.3c01158
ACS Omega 2023, 8, 15650−15659

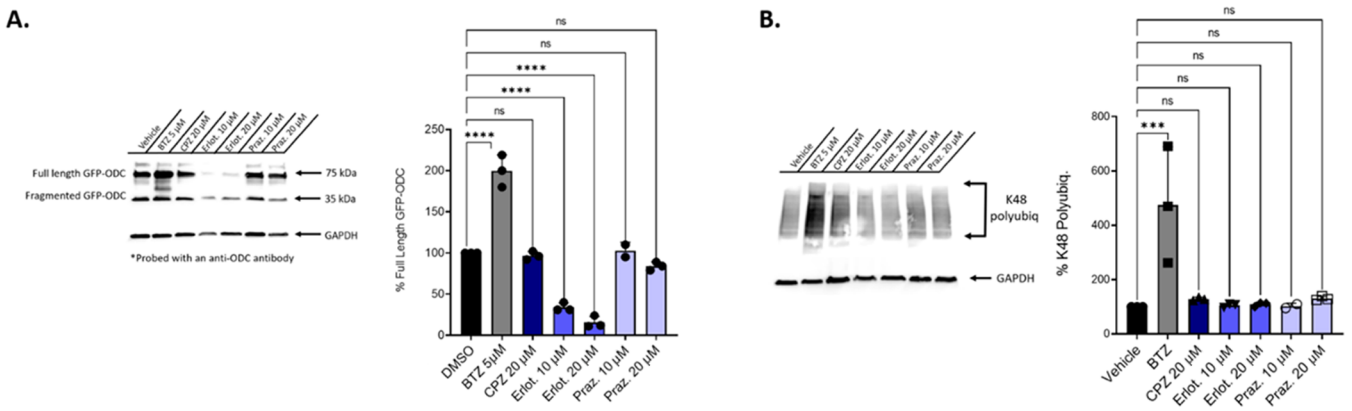

Figure 6. (A) Degradation of GFP-ODC by the lead hits, visualized and quantified using a western blot. There were two significant bands identified. The band at 75 kDa was identified as the full-length GFP-ODC, and the band at 35 kDa is predominantly GFP, with a small fragment of ODC remaining. Cells were treated with 10 or 20 μM erlotinib and prazosin. As controls, 5 μM of a proteasome inhibitor, Bortezomib (BTZ), was used, and 20 μM CPZ was added. Quantification of the full-length GFP-ODC was done in triplicate. (B) Effects of overall ubiquitinoylation in cells that are treated with erlotinib, prazosin, and CPZ. Quantification of α-synuclein degradation by each compound was done in triplicate. One-way ANOVA statistical analysis was used to determine statistical significance. ns = not significant, $*p < 0.05$, $**p < 0.01$, $***p < 0.001$, $****p < 0.0001$, with error bars denoting SD.

signal with low cytotoxicity but were unable to reduce the signal by 50% (Figure 4D,E). The 8-point titration curves of the remaining six compounds and CPZ are displayed in Figure S2. Two compounds, homoharringtonine and triptolide, significantly decreased the AlphaLISA signal but not in a dose-dependent manner. Homoharringtonine and triptolide are both natural products that have been evaluated for the treatment of a variety of cancers, and both natural products inhibit the expression of proteins.[47,48] Homoharringtonine inhibits protein translation by preventing the initial elongation step through the interaction with the ribosomal A-site,[47] while triptolide inhibits RNA polymerase II-mediated transcription (Figure S2).[48] Although these two compounds will not become lead compounds, they do represent great controls for our screen and emphasize the importance of orthogonal assays to validate our lead compounds. The remaining compounds, prazosin, thiothixene, bromocriptine, and fluoxetine, did not reduce the AlphaLISA signal below 50% (Figure S2) or did not reduce the AlphaLISA signal without significant cell death.

To ensure direct activation of the 20S proteasome was occurring, the 20S proteasome activities of all 5 compounds and CPZ (as a control) were assessed by utilizing the standard fluorogenic 7-amino-methylcoumarin (AMC) in a purified proteasome assay. The conjugated small peptide substrates that correspond to each one of the catalytic sites in the 20S proteasome were used, chymotrypsin-like site (Suc-LLVY-AMC), caspase-like site (Z-LLE-AMC), and trypsin-like site (Boc-LRR-AMC).[27] Once the peptides enter into the 20S proteasome and interact with the catalytic sites, the AMC probe is cleaved, releasing a fluorescent signal. The 20S proteasome was treated with a range of concentrations of the compounds and a vehicle control and subsequently incubated at 37 °C for 20 min. After incubation, an equimolar mixture of the three fluorogenic peptide probes (13.3 μM of each) was added, and the fluorescent output was recorded every 5 min for an hour. The rate of 20S proteasome-mediated proteolysis induced by the small molecules is evaluated at varying concentrations to determine the concentration at which the rate of proteolysis was doubled compared to the vehicle control (hereafter named as EC_{200}). Compounds were added to wells that contained 1 nM of purified human 20S proteasome in an 8-point titration with concentrations ranging from 1.25 to 80 μM. The compounds that were deemed active were retested at a 10-point concentration titration of 0.32 to 80 μM.

Of the 5 compounds evaluated for purified 20S proteasome activation, only erlotinib had an EC_{200} at 12 μM (Figure 5A), satisfying our final screening funnel criteria (Figure 3, EC_{200} < 20 μM). Prazosin was also evaluated for the 20S proteasome enhancement due to the structural similarity to erlotinib (Figure 5C,D). The 20S proteasome treated with erlotinib and prazosin displayed a max fold increase of 5.7 and 4.5, respectively. Of the three catalytic sites in the 20S proteasome, CPZ only activated the chymotrypsin-like site while having an overall max-fold increase of 6.3.[22] The three catalytic sites in the 20S proteasome allosterically communicate with one another.[28] CPZ's selective activation of a single-site may interfere with its ability to effectively cleave the GFP-ODC substrate. Unlike CPZ, both prazosin and erlotinib were observed to activate more than one catalytic site. Prazosin activated two catalytic sites: the caspase-like site (max fold increase of 5.8) and the chymotrypsin-like site (max fold increase of 3.5) (Figure S3). Erlotinib, however, activated the trypsin-like, chymotrypsin-like, and caspase-like sites, with max fold increase of 5.9, 5.1, and 3.1, respectively (Figure S3). The activities of the remaining 4 compounds are depicted in Figure S3.

The selectivity of these three compounds for purified 20S proteasome over purified 26S proteasome was then evaluated, using the same fluorogenic small peptide assay. Only at the highest concentration, erlotinib and prazosin were able to modestly activate the 26S proteasome between 2.5- to 3-fold, while CPZ only enhanced the 26S proteasome 2-fold (Figure 5B), indicating that the primary enhanced proteolytic activity resides with the 20S proteasome.

Due to its efficient proteasome enhancement *in vitro*, erlotinib was the most promising novel proteasome enhancer. To determine whether the proteasome activity displayed by erlotinib translates to a full-length and pathologically relevant protein, we evaluated whether erlotinib-treated 20S proteasome enhances α-synuclein degradation *in vitro*. We treated

https://doi.org/10.1021/acsomega.3c01158
ACS Omega 2023, 8, 15650−15659

purified 20S proteasome with two concentrations of erlotinib (10 and 20 μM) and a DMSO control. After a 45 min incubation at 37 °C, purified α-synuclein was added, and the mixture was incubated for an additional 3 h. The levels of α-synuclein were visualized and quantified using a western blot, and the level of GAPDH was used as the loading control. As compared to the untreated proteasome, the samples treated with 10 μM erlotinib had 68% α-synuclein remaining. The proteasome that was incubated with 20 μM erlotinib had 48% α-synuclein remaining. This indicates that erlotinib's ability to enhance the proteolytic activity of the proteasome translates to full-length IDPs other than ODC (Figure 5E).

Finally, the ability of erlotinib to enhance the degradation of ODC in an assay orthogonal to the AlphaLISA was evaluated. This assay was conducted to verify the mechanism of the reduction of the AlphaLISA signal seen by the lead compounds. The HEK-293T that stably expressed the conjugated GFP-ODC used in the high-throughput screen was treated with two concentrations of erlotinib and prazosin (10 and 20 μM), 20 μM CPZ, and 5 μM of a proteasome inhibitor, Bortezomib (BTZ). CPZ was used again to directly compare the hits from the two screens, while BTZ was used as a negative control. The levels of GFP-ODC were visualized and quantified using a western blot with the band at 75 kDa representing the full-length conjugated protein and the band at 35 kDa a fragment of GFP-ODC (Figure 6A); only the full-length protein band was quantified. Both concentrations of prazosin and the CPZ control did very little in enhancing the degradation of ODC. CPZ had 97% of the full-length GFP-ODC remaining, and prazosin at the same concentration had 84% of ODC remaining. Erlotinib, in contrast, showed a significant enhancement in the degradation of the full-length GFP-ODC. At 10 μM, only 34% of the intact conjugated protein remained, while at 20 μM, only 16% remained (Figure 6A). To ensure we were solely observing 20S proteasome activation, we evaluated ubiquitin levels in the same cell lysates (Figure 6B). None of the compounds had any effect on K48 ubiquitin except for the proteasome inhibitor, BTZ. This supports that erlotinib does not impact the ubiquitin-dependent pathway but rather enhances degradation through the ubiquitin-independent pathway.

CONCLUSIONS

The UPS is responsible for the degradation of most intracellular and soluble proteins.[3,4,7] Dysregulation of the expression or degradation of proteins, including IDPs, can cause fatal cellular system failures.[16] Recently, enhancement of the 20S proteasome has provided a promising therapeutic pathway for diseases such as neurodegeneration and cancers such as multiple myeloma.[19−22,24] Despite the potential of this innovative therapeutic pathway, limited cell-based high-throughput assays are available to identify novel proteasome modulators. Herein, we describe the successful optimization of a cell-based AlphaLISA assay that evaluates the increased or decreased degradation of ODC, a model IDP. We readily modified this AlphaLISA assay to meet the demands of a high-throughput screen and successfully screened two compound libraries: the Prestwick and NIH Clinical Libraries. From this screening, we identified 11 hit compounds. From these 11 compounds, only erlotinib was identified as a new 20S proteasome enhancer. While erlotinib is an EGFR tyrosine kinase inhibitor, the reported IC_{50} for this activity is 2 nM,[39] which is drastically lower than the IC_{50} of 5.4 μM in the AlphaLISA. This suggests that the increased proteolytic degradation of ODC is not through the EGFR activity of erlotinib, which was confirmed using a purified 20S proteasome assay. Erlotinib was able to enhance all three catalytic sites of the 20S proteasome with an overall max fold increase of 5.7. This activity translated to the enhanced proteolytic degradation of purified full-length α-synuclein with 68% α-synuclein remaining in samples treated with 10 μM erlotinib and only 48% remaining when treated with 20 μM erlotinib. This proteasome enhancement was selective for the 20S proteasome, as displayed both in the purified small peptide assay and in the HEK-293T cells expressing GFP-ODC. While both 10 and 20 μM erlotinib readily enhanced the degradation of ODC (34 and 16% remaining, respectively), it had no impact on the levels of ubiquitinylated proteins, making erlotinib the only lead compound identified. The development of this AlphaLISA assay will readily allow for the identification of novel proteasome modulators, such as erlotinib. This class of compounds can then be further developed to diminish any non-proteasome-related biological activity and allow for the synthesis of more potent and efficient 20S proteasome enhancers.

EXPERIMENTAL SECTION

GFP-ODC Transfection. HEK-293T cells were seeded at a density of 1×10^5 cells/mL in a 24-well plate overnight. DNA (1 μg of GFPSpark-ODC plasmid) was mixed with 250 μL of serum-free Dulbecco's modified Eagle's medium (DMEM). Sinofection transfection reagent (5 μL) was mixed with 250 μL of serum-free DMEM in a separate vial. The two vials were then combined and incubated at room temperature for 15 min. The mixture was then added to the HEK-293T cells in the 24-well plate and incubated for 4 h at 37 °C with 5% CO_2. After this incubation, the media was replaced with fresh DMEM. After 3 days, cells were removed from the plate with trypsin (0.25%) and resuspended in hygromycin selection media (100 μg/mL). The surviving clones were picked and expanded in the selection media for 6 weeks. After three passages, stable expression was confirmed by confocal fluorescent imaging using standard GFP filters. The stable clones were then further sorted using flow cytometry using the standard GFP filters to make pools of "high" and "medium" GFP expressors.

Bead Concentration Optimization. HEK-293T cells that transiently expressed GFP-ODC were seeded at 500 cells/well in a solid-bottom white 384-well plate in 20 μL of DMEM for 12 h. The cells were then lysed with 5 μL of the AlphaLISA lysis buffer. The lysate was then diluted in the 1× AlphaLISA immunoassay buffer to the desired 10× final concentration. 5 μL of each sample was transferred into a solid-bottom white 384-well plate. Then, 10 μL of the anti-GFP acceptor bead and biotinylated anti-ODC were added in different ratios and incubated for 1 h at room temperature. After this incubation, 25 μL of the donor beads were added for each of the screened concentrations and incubated for a further 30 min. The AlphaLISA signal was measured using the BioTek plate reader equipped with an α filter.

AlphaLISA. HEK-293T cells that stably expressed GFP-ODC were plated at 10,000 cells/well in a 384-well plate in 20 μL of phenol red-free DMEM. The cells were then immediately treated with either DMSO or TCH-165. After 18 h, 5 μL of the 5× AlphaLISA Surefire lysis buffer was added to each well, and then the plate was incubated on a shaker (400 rpm) at room temperature for 30 min. During this first

https://doi.org/10.1021/acsomega.3c01158
ACS Omega 2023, 8, 15650−15659

incubation, a 10× mix of either a mixture of biotinylated anti-ODC (4.7 μg/mL) and anti-GFP (100 μg/mL) in 1× AlphaLISA immunoassay buffer or just anti-GFP (100 μg/mL) in 1× AlphaLISA immunoassay buffer was made under limited light conditions. After the lysis was complete, 5 μL of either mixture was added to each well using an automated dispenser. After this addition, the plate was incubated at room temperature and in the dark for 1 h. Then, a 2.5× mix was made with the streptavidin donor bead (100 μg/mL) in 1× AlphaLISA immunoassay buffer in a limited fluorescent light setting. From this 2.5× mix, 20 μL was added to each well using the automated dispenser, and the plate was incubated again at room temperature in the dark for 30 min. The AlphaLISA signal was measured using BioTek plate reader equipped with an α filter.

TrueHits Screen. In the white 384-well assay plate, 20 μL of clear DMEM was added. Then, a 1.7× stock solution of Biotin (final concentration of 10 μM) was added. The desired drugs were then added at the same concentration that the screen was run (15 μM). 5× of the AlphaLISA donor bead stock was then added (for a final concentration of 10 μg/mL) and incubated for 1 h at room temperature. Then, a 5× solution of the AlphaLISA acceptor bead was added (final concentration of 10 μg/mL), and the mixture was incubated in the dark for 30 min at room temperature. The AlphaLISA signal was measured using BioTek plate reader equipped with an α filter.

Small Peptide Assay. Activity assays were carried out in a 100 μL reaction volume using a black flat/clear bottom 96-well plate. Different concentrations (1.25−80 μM) of test compounds were added to the wells containing 1 nM of human constitutive 20S proteasome in a 38 mM Tris-HCl and 100 mM NaCl buffer at a pH of 7.8. The mixture was allowed to incubate for 15 min at 37 °C. After this incubation, 5 μL of the fluorogenic substrates were added. The fluorogenic substrates used were either one of the following or a combination of all three (final concentration of 6.67 μM of each): Suc-LLVY-AMC (CT-L activity, final concentration of 20 μM), Z-LLE-AMC (Casp-L activity, final concentration of 20 μM), Boc-LRR-AMC (T-L activity, final concentration of 40 μM). The activity was measured at 37 °C on a SpectraMax M5e spectrometer by measuring the change in fluorescence unit per minute for 1 h at 380−460 nm. The rate of hydrolysis for the vehicle control was set at 100%, and the ratio of the treated sample over the vehicle control was used to calculate the fold change in the rate of substrate hydrolysis by the proteasome. The same protocol was used for the activity assays involving the 26S proteasome, but 2.5 mM ATP and 5 mM Magnesium chloride were added to the assay buffer in place of NaCl.

***In Vitro* Degradation of α-Synuclein.** Degradation assays were carried out in a 25 μL reaction volume using a 50 mM HEPES and 5 mM DTT buffer at a pH of 7.2, 0.3 μM of purified α-synuclein, and 10 nM of purified human 20S proteasome. The 20S proteasome was first diluted to 45.5 nM in the HEPES buffer, and 0.5 μL of the test compounds or DMSO was added. This mixture was incubated for 45 min at 37 °C. After this incubation, 2.5 μL of a 15 μM stock of α-synuclein was added. The degradation mixture was incubated at 37 °C for 3 h, and then 0.5 μM GAPDH was added as a loading control. The reaction was stopped with the addition of concentrated SDS loading buffer and boiled for 20 min. The samples were then resolved on a 4−20% Tris-glycine SDS-PAGE gel and immunoblotted with mouse monoclonal anti-α-synuclein IgG (1:2000) and anti-mouse HRP-linked IgG (1:2000). The immunoblots were developed with ECL Western reagent and imaged with an Azure Biosystems 300Q imager.

Cellular Degradation of GFP-ODC. In 60 mm plates, HEK-293T cells that stably expressed GFP-ODC were grown to 80% confluency. Then, the cells were treated with 3 μL of either DMSO or the test compound at the desired concentration. The cells were treated for 16 h and then scraped and pelleted (300 g for 5 min). The supernatant was taken off, and the cell pellet was washed with ice-cold PBS and then lysed with a RIPA buffer containing protease inhibitors. The cell lysate was incubated for 20 min on ice. The lysate was centrifuged for 15 min at 500*g*, and then the supernatant was collected. Concentrated SDS loading buffer was added, and the samples were boiled for 10 min. The samples were then resolved on a 4−20% Tris-glycine SDS-PAGE gel and immunoblotted with mouse monoclonal anti-ODC IgG (1:2000) and anti-mouse HRP-linked IgG (1:2000). The immunoblots were developed with ECL western reagent and imaged with an Azure Biosystems 300Q imager.

■ ASSOCIATED CONTENT

Supporting Information

The Supporting Information is available free of charge at https://pubs.acs.org/doi/10.1021/acsomega.3c01158.

> Assay optimization conditions; titration curves of AlphaLISA; cell viability assays; fluorogenic peptide assays; replicates of western blots of purified α-synuclein; and replicates of western blots of GFP-ODC and ubiquitin in HEK293Tcells (PDF)

■ AUTHOR INFORMATION

Corresponding Author

Jetze J. Tepe − *Department of Chemistry and Department of Pharmacology and Toxicology, Michigan State University, East Lansing, Michigan 48824, United States;* orcid.org/0000-0001-5467-5589; Email: Tepe@chemistry.msu.edu

Authors

Sophia D. Staerz − *Department of Chemistry and Department of Pharmacology and Toxicology, Michigan State University, East Lansing, Michigan 48824, United States*

Erika M. Lisabeth − *Department of Pharmacology and Toxicology, Michigan State University, East Lansing, Michigan 48824, United States*

Evert Njomen − *Department of Chemistry and Department of Pharmacology and Toxicology, Michigan State University, East Lansing, Michigan 48824, United States*

Thomas S. Dexheimer − *Department of Pharmacology and Toxicology, Michigan State University, East Lansing, Michigan 48824, United States*

Richard R. Neubig − *Department of Pharmacology and Toxicology, Michigan State University, East Lansing, Michigan 48824, United States;* orcid.org/0000-0003-0501-0008

Complete contact information is available at: https://pubs.acs.org/10.1021/acsomega.3c01158

https://doi.org/10.1021/acsomega.3c01158
ACS Omega 2023, 8, 15650−15659

Author Contributions

S.D.S. optimized the AlphaLISA assay and conducted the high-throughput screen with E.M.L. S.D.S conducted all of the orthogonal assays to identify lead compounds and wrote the bulk of the manuscript. E.N. and T..D. conceived the idea of using the AlphaLISA to identify novel proteasome modulators and performed initial preliminary validation assays and the reagent optimization assay. J.J.T. and R.R.N. provided guidance for data evaluation and aided in the writing of the manuscript. All authors have given approval to the final version of the manuscript.

Funding

The National Institutes of Health, NS111347 and the National Institute of General Medical Sciences, T32GM092715 of the National Institutes of Health.

Notes

The authors declare the following competing financial interest(s): J.T.T. has a competing interest due to his involvement with Portera Therapeutics. The other authors have no conflict of interests.

■ ACKNOWLEDGMENTS

The authors gratefully acknowledge financial support from the National Institutes of Health, National Institute of Neurological Disorders and Stroke. The authors would also like to acknowledge the help of Daniel Vocelle and the Flow Cytometry core at Michigan State University for all of the help and guidance during the cell sorting.

■ ABBREVIATIONS USED

AlphaLISA, amplified luminescent proximity homogeneous assay; AMC, 7-amino-4-methylcoumarin; ATP, adenosine triphosphate; α-syn, α-synuclein; BTZ, bortezomib; C-L, caspase-like; CHX, cycloheximide; CPZ, chlorpromazine; CT-L, chymotrypsin-like; DMEM, Dulbecco's modified Eagle's medium; DMSO, dimethyl sulfoxide; DTT, dithiothreitol; ECL, enhanced chemiluminescence; GFP, green fluorescent protein; HEK293T, human embryonic kidney cells; HRP, horseradish peroxidase; IDP, intrinsically disordered protein; ODC, ornithine decarboxylase; PBS, phosphate buffered saline; Parkinson's disease; RIPA, radioimmunoprecipitation assay; SDS, sodium dodecyl sulfate; T-L, trypsin-like; UPS, ubiquitin−proteasome system

■ REFERENCES

(1) Hipp, M. S.; Kasturi, P.; Hartl, F. U. The proteostasis network and its decline in ageing. *Nat. Rev. Mol. Cell Biol.* **2019**, *20*, 421−435.
(2) Hegde, A. N.; Upadhya, S. C. The ubiquitin-proteasome pathway in health and disease of the nervous system. *Trends Neurosci.* **2007**, *30*, 587−595.
(3) Thibaudeau, T. A.; Smith, D. M. A practical review of pharmacology. *Pharmacol. Rev.* **2019**, *71*, 170−197.
(4) George, D. E.; Tepe, J. J. Advances in proteasome enhancement by small molecules. *Biomolecules* **2021**, *11*, No. 1789.
(5) Njomen, E.; Tepe, J. J. Proteasome activation as a new therapeutic approach to target proteotoxic disorders. *J. Med. Chem.* **2019**, *62*, 6469−6481.
(6) Jones, C. L.; Tepe, J. J. Proteasome activation to combat proteotoxicity. *Molecules* **2019**, *24*, No. 2841.
(7) Tanaka, K. The proteasome: overview of structure and functions. *Proc. Jpn. Acad., Ser. B* **2009**, *85*, 12−36.
(8) Bard, J. A. M.; Goodall, E. A.; Greene, E. R.; Jonsson, E.; Dong, K. C.; Martin, A. Structure and function of the 26S Proteasome. *Annu. Rev. Biochem.* **2018**, *87*, No. 697.
(9) Orlowski, M.; Wilk, S. Catalytic Activities of the 20S proteasome, a multicatalytic proteinase complex. *Arch. Biochem. Biophys.* **2000**, *383*, 1−16.
(10) Ben-Nissan, G.; Sharon, M. Regulating the 20S Proteasome ubiquitin-independent degradation pathway. *Biomolecules* **2014**, *4*, 862−884.
(11) Deshmukh, F. K.; Yaffe, D.; Olshina, M. A.; Ben-Nissan, G.; Sharon, M. The contribution of the 20S proteasome to proteostasis. *Biomolecules* **2019**, *9*, No. 190.
(12) Bhattarai, A.; Emerson, I. A. Dynamic conformational flexibility and molecular interactions of intrinsically disordered proteins. *J. Biosci.* **2020**, *45*, No. 29.
(13) Zhang, Y.; Cao, H.; Liu, Z. Binding cavities and druggability of intrinsically disordered proteins. *Protein Sci.* **2015**, *24*, 688−705.
(14) Hervás, R.; Oroz, J. Mechanistic insights into the role of molecular chaperones in protein misfolding diseases: from molecular recognition to amyloid disassembly. *Int. J. Mol. Sci.* **2020**, *21*, No. 9186.
(15) Conway, K. A.; Harper, J. D.; Lansbury, P. T. Accelerated in vitro fibril formation by a mutant alpha-synuclein linked to early-onset Parkinson disease. *Nat. Med.* **1998**, *4*, 1318−1320.
(16) Thibaudeau, T. A.; Anderson, R. T.; Smith, D. M. A common mechanism of proteasome impairment by neurodegenerative disease-associated oligomers. *Nat. Commun.* **2018**, *9*, No. 1097.
(17) Fares, M. B.; Jagannath, S.; Lashuel, H. A. Reverse engineering Lewy bodies: how far have we come and how far can we go? *Nat. Rev. Neurosci.* **2021**, *22*, 111−131.
(18) Kalkat, M.; De Melo, J.; Hickman, K. A.; Lourenco, C.; Redel, C.; Resetca, D.; Tamachi, A.; Tu, W. B.; Penn, L. Z. MYC deregulation in primary human cancers. *Genes* **2017**, *8*, No. 151.
(19) Njomen, E.; Vanecek, A.; Lansdell, T. A.; Yang, Y. T.; Schall, P. Z.; Harris, C. M.; Bernard, M. P.; Isaac, D.; Alkharabsheh, O.; Al-Janadi, A.; Giletto, M. B.; Ellsworth, E.; Taylor, C.; Tang, T.; Lau, S.; Bailie, M.; Bernard, J. J.; Yuzbasiyan-Gurkan, V.; Tepe, J. J. Small Molecule 20S proteasome enhancer regulates MYC protein stability and exhibits antitumor activity in Multiple Myeloma. *Biomedicines* **2022**, *10*, No. 938.
(20) Fiolek, T. J.; Magyar, C. L.; Wall, T. J.; Davies, S. B.; Campbell, M. V.; Savich, C. J.; Tepe, J. J.; Mosey, R. A. Dihydroquinazolines enhance 20S proteasome activity and induce degradation of alpha-synuclein, an intrinsically disordered protein associated with neurodegeneration. *Bioorg. Med. Chem. Lett.* **2021**, *36*, No. 127821.
(21) Fiolek, T. J.; Keel, K. L.; Tepe, J. J. Fluspirilene analogs activate the 20S proteasome and overcome proteasome impairment by intrinsically disordered protein oligomers. *ACS Chem. Neurosci.* **2021**, *12*, 1438−1448.
(22) Jones, C. L.; Njomen, E.; Sjogren, B.; Dexheimer, T. S.; Tepe, J. J. Small molecule enhancement of 20S proteasome activity targets intrinsically disordered proteins. *ACS Chem. Biol.* **2017**, *12*, 2240−2247.
(23) Njomen, E.; Osmulski, P. A.; Jones, C. L.; Gazynska, M.; Tepe, J. T. Small molecule modulation of proteasome assembly. *Biochemistry* **2018**, *57*, 4214−4224.
(24) Staerz, S. D.; Jones, C. L.; Tepe, J. J. Design, synthesis, and biological evaluation of potent 20S proteasome activators for the potential treatment of alpha-synucleinopathies. *J. Med. Chem.* **2022**, *65*, 6631−6642.
(25) Osmulski, P. A.; Karpowicz, P.; Jankowska, E.; Bohmann, J.; Pickering, A. M.; Gaczynska, M. New peptide-based pharmacophore activates 20S proteasome. *Molecules* **2020**, *25*, No. 1439.
(26) Coleman, R. A.; Muli, C. S.; Zhao, Y.; Bhardwaj, A.; Newhouse, T. R.; Trader, D. J. Analysis of chain length, substitution patterns, and unsaturation of AM-404 derivatives as 20S proteasome stimulators. *Bioorg. Med. Chem. Lett.* **2019**, *29*, 420−423.
(27) Trader, D. J.; Simanski, S.; Dickson, P.; Kodadek, T. Establishment of a suite of assays that support the discovery of proteasome stimulators. *Biochim. Biophys. Acta, Gen. Subj.* **2017**, *1861*, 892−899.

https://doi.org/10.1021/acsomega.3c01158
ACS Omega 2023, 8, 15650−15659

(28) Kisselev, A. F.; Goldberg, A. L. *Monitoring Activity and Inhibition of 26S Proteasomes with Fluorogenic Peptide Substrates*; Elsevier, 2005; p 364.
(29) Zerfas, B. L.; Coleman, R. A.; Salazar-Chaparro, A. F.; Macatangay, N. J.; Trader, D. J. Fluorescent probes with unnatural amino acids to monitor proteasome activity in real-time. *ACS Chem. Biol.* **2020**, *15*, 2588−2596.
(30) Gan, J.; Leestemaker, Y.; Sapmaz, A.; Ovaa, H. Highlighting the proteasome: using fluorescence to visualize proteasome activity and distribution. *Front. Mol. Biosci.* **2019**, *6*, No. 14.
(31) Coleman, R. A.; Trader, D. J. Development and application of a sensitive peptide reporter to discover 20S proteasome stimulators. *ACS Comb. Sci.* **2018**, *20*, 269−276.
(32) Coleman, R. A.; Trader, D. J. A sensitive high-throughput screening method for identifying small molecule stimulators of the core particle of the proteasome. *Curr. Protoc. Chem. Biol.* **2018**, *10*, No. e52.
(33) Meng, L.; M, R.; Kwok, B. H. B.; Elofsson, M.; Sin, N.; Crews, C. M. Epoxomicin, a potent and selective proteasome inhibitor, exhibitsin vivoantiinflammatory activity. *Proc. Natl. Acad. Sci. U.S.A.* **1999**, *96*, 10403−10408.
(34) Bragança, C. E.; Kraut, D. A. Mode of targeting to the proteasome determines GFP fate. *J. Biol. Chem.* **2020**, *295*, 15892−15901.
(35) Kahana, C.; Asher, G.; Shaul, Y. Mechanisms of protein degradation: an odyssey with ODC. *Cell Cycle* **2005**, *4*, 1461−1464.
(36) Bielefeld-Sevigny, M. AlphaLISA immunoassay platform- the ″no-wash″ high-throughput alternative to ELISA. *Assay Drug Dev. Technol.* **2009**, *7*, 90−92.
(37) Prabhu, L.; Chen, L.; Wei, H.; Demir, O.; Safa, A.; Zeng, L.; Amaro, R. E.; O'Neil, B. H.; Zhang, Z. Y.; Lu, T. Development of an AlphaLISA high throughput technique to screen for small molecule inhibitors targeting protein arginine methyltransferases. *Mol. BioSyst.* **2017**, *13*, 2509−2520.
(38) Ishii, K. Functional singlet oxygen generators based on pthalocyanines. *Coord. Chem. Rev.* **2012**, *256*, 1556−1568.
(39) Mai, E.; Wong, W. L.; Bennett, G.; Billeci, K. Comparison of ELISA and Alphascreen assay technologies for measurement of protein expression levels. *PerkinElmer Application Note*, 2002.
(40) Goktug, A. N.; Chai, S. C.; Chen, T. Data Analysis Approaches in High Throughput Screening. In *Drug Discovery*; InTechOpen, 2013.
(41) Zhang, J. H.; Chung, T. D.; Oldenburg, K. R. A simple statistical parameter for use in evaluation and validation of high throughput screening assays. *SLAS Discovery* **1999**, *4*, 67−73.
(42) Hartman, P. E.; Levine, K.; Hartman, Z.; Berger, H. Hycanthone: a frameshift mutagen. *Science* **1971**, *172*, 1058−1060.
(43) Moyer, J. D.; Barbacci, E. G.; Iwata, K. K.; Arnold, L.; Boman, B.; Cunningham, A.; DiOrio, C.; Doty, J.; Reynolds, M. M.; Sloan, D.; Theleman, A.; Miller, P. Induction of apoptosis and cell cycle arrest by CP-358,774, an inhibitor of Epidermal Growth Factor Receptor Tyrosine Kinase. *Cancer Res.* **1997**, *57*, 4838−4848.
(44) Van Dyke, K.; Lantz, C.; Szustkiewicz, C. Quinacrine: mechanisms of antimalarial action. *Science* **1970**, *169*, 492−493.
(45) Gabbard, R. D.; Hoopes, R. R.; Kemp, M. G. Spironolactone and XPB: An old drug with a new molecular target. *Biomolecules* **2020**, *10*, No. 756.
(46) Covaci, O.-I.; Mitran, R.-A.; Buhalteanu, L.; Dumitrescu, D. G.; Shova, S.; Manta, C.-M. Bringing new life into old drugs: a case study on nifuroxazide polymorphism. *CrystEngComm* **2017**, *19*, 3584−3591.
(47) Lü, S.; Wang, J. Homoharringtonine and omacetaxine for myeloid hematological malignancies. *J. Hematol. Oncol.* **2014**, *7*, No. 2.
(48) Titov, D. V.; Gilman, B.; He, Q. L.; Bhat, S.; Low, W. K.; Dang, Y.; Smeaton, M.; Demain, A. L.; Miller, P. S.; Kugel, J. F.; Goodrich, J. A.; Liu, J. O. XPB, a subunit of TFIIH, is a target of the natural product triptolide. *Nat. Chem. Biol.* **2011**, *7*, 182−188.

https://doi.org/10.1021/acsomega.3c01158
ACS Omega 2023, 8, 15650−15659